

## Cylindrical paraxial optical beams described by the incomplete gamma function

Tomasz Radożycki <sup>\*</sup>

Faculty of Mathematics and Natural Sciences, College of Sciences, Institute of Physical Sciences,  
Cardinal Stefan Wyszyński University, Wóycickiego 1/3, 01-938 Warsaw, Poland



(Received 24 September 2021; accepted 11 November 2021; published 24 November 2021)

An analytic formula for a certain type of a cylindrical beam, which might be called a  $\gamma$  beam, has been derived directly from the paraxial equation and independently using the method of the Hankel transform formulated in our previous work [T. Radożycki, *Opt. Laser Technol.* **147**, 107670 (2022)]. The fundamental properties of this beam are analyzed and the parameters characterizing the beam shape are identified. The connection with Gaussian and elegant Laguerre-Gauss beams is demonstrated. In the plane perpendicular to the propagation axis, this beam is shown to display an expanding ring of high-energy concentration. At large radial distances the spatial profile exhibits a power-law falloff. The phase of the wave is also studied in this paper. Close to the symmetry axis it is shown to be typical of modes that exhibit vortex character, such as Gaussian beams of  $n$ th order, but at large distances it reveals a peculiar behavior distinct from Gaussian-type beams.

DOI: [10.1103/PhysRevA.104.053528](https://doi.org/10.1103/PhysRevA.104.053528)

### I. INTRODUCTION

For a number of years, physics of optical laser beams has attracted the attention of researchers due to its numerous and important applications among which one can mention optical trapping and guiding of particles, image processing, optical communication, harmonics generation in nonlinear optics, quantum cryptography, and even those outside the direct concern of physics, such as biology and medicine [1–12], but the full range of applications is very wide.

An important class constitutes beams exhibiting cylindrical symmetry, in particular those that are solutions to the paraxial wave equation. Of those for which rigorous analytical expressions have been found, and which therefore draw special interest from a theoretical point of view, one should mention pure Gaussian (G) beams [13–22], Bessel-Gauss (BG) beams, hyperbolic BG and “special” hyperbolic BG beams [22–28], as well as Laguerre-Gauss (LG) beams [14,22,25,29–33], a number of which exhibit a ringlike pattern of irradiance in the transverse plane and are endowed with vorticity “charge.”

It should be emphasized that these examples are realistic. Their structure, far from the trivial, idealized, and purely textbook case of plane waves, can lead to various intriguing phenomena which call for, and certainly shall find, a wide range of practical applications. The current paper fits into this line of issues. It is devoted to the description of a certain type of optical beams, for which the name “ $\gamma$  beams” seems adequate, and which are again exact solutions of the paraxial Helmholtz equation, but apparently have not been dealt with in the literature. Their existence was briefly mentioned in our previous work devoted to a different topic [34], but a detailed examination was left as the focus of the present paper. Below we derive their analytical form step by step and investigate

the basic properties. These beams do not display any Gaussian falloff but for  $n > 1$  (where  $n$  stands for vorticity) they are still square integrable in the transverse plane and, therefore, do not constitute merely an academic example.

The findings of this paper are derived within the framework of the standard scalar and paraxial approximations of Maxwell equations. The wave propagating along the  $z$  axis is then represented with a scalar function

$$\Psi(\mathbf{r}, z, t) = e^{ik(ct-z)}\psi(\mathbf{r}, z), \quad (1)$$

where the envelope  $\psi(\mathbf{r}, z)$  satisfies the paraxial equation:

$$\Delta_{\perp}\psi(\mathbf{r}, z) + 2ik\partial_z\psi(\mathbf{r}, z) = 0. \quad (2)$$

The Laplace operator  $\Delta_{\perp}$  stands here for a two-dimensional one acting in the transverse plane only, and  $\partial_z$  denotes the partial derivative  $\frac{\partial}{\partial z}$ . The details of the above approximations are given elsewhere [14,35].

In polar coordinates  $r = \sqrt{x^2 + y^2}$  and  $\varphi$ , that are particularly suitable for our purposes, the dependence on the angular variable can be isolated by means of the substitution

$$\psi(r, \varphi, z) = e^{in\varphi}\Phi(r, z), \quad \text{where } n \in \mathbb{Z}, \quad (3)$$

and the paraxial equation can be finally given the form

$$\left(\partial_r^2 + \frac{1}{r}\partial_r - \frac{n^2}{r^2} + 2ik\partial_z\right)\Phi(r, z) = 0. \quad (4)$$

A special analytical solution to this equation will be derived in the next section and a couple of basic properties will be indicated. In Sec. III we will study the parameters characterizing the beam under consideration. Since at large distances the beam’s behavior is not Gaussian, these parameters will be defined *ab initio*. Finally, Sec. IV is devoted to the analysis of the intensity and phase distributions both in the transverse and axial planes.

\*t.radozycki@uksw.edu.pl

**II. DERIVATION OF THE FORMULA FOR  $\gamma$  BEAMS**

In order to find the desired solution, the function  $\Phi(r, z)$  is substituted into (4) in the form of

$$\Phi(r, z) = \frac{1}{r^n} \chi(r, z). \tag{5}$$

Simple and straightforward transformations lead to the following equation for the function  $\chi(r, z)$ :

$$\partial_r^2 \chi(r, z) + \frac{1-2n}{r} \partial_r \chi(r, z) + 2ik \partial_z \chi(r, z) = 0. \tag{6}$$

Now, to solve it one can observe that when introducing a new complex variable  $u$  as

$$u = \frac{r^2}{a + iz}, \tag{7}$$

with  $a$  being a constant to be fixed later, the following differential equation for  $\chi(u)$  is obtained:

$$\chi''(u) + \frac{1-n}{u} \chi'(u) + \frac{k}{2} \chi(u) = 0. \tag{8}$$

The separate dependence on  $r$  and  $z$  has disappeared and, contrary to (6), one has now to do with an *ordinary* differential equation. Obviously, primes stand here for the differentiations with respect to  $u$ . This equation can easily be solved in two steps when substituting a certain new function for  $\chi'(u)$ . Leaving aside rather obvious computational details, it is readily found that the solution of (8) has the form

$$\chi(u) = C \left(\frac{2}{k}\right)^n \gamma\left(n, \frac{ku}{2}\right) + \tilde{C}, \tag{9}$$

where  $\gamma$  denotes the (*lower*) *incomplete gamma function* [36].

Since (8) is a homogeneous equation and only derivatives of  $\chi(u)$  appear, neither constant  $C$  nor  $\tilde{C}$  can be fixed at this stage. The latter is simply set to zero in order to get a normalizable solution. As regards the former, it will be found later via the normalization condition. Consequently one obtains

$$\Phi(r, z) = C \left(\frac{2}{k}\right)^n \frac{1}{r^n} \gamma\left(n, \frac{kr^2}{2(a + iz)}\right). \tag{10}$$

It can be assumed that  $a$  is real since any eventual imaginary part merely shifts the variable  $z$ . Moreover, the normalization condition of the beam in the perpendicular plane requires  $a$  to be positive, since otherwise the function would be exponentially growing with  $r^2$ . Denoting  $2a/k =: w_0^2$ , one gets the final expression

$$\Phi(r, z) = C \left(\frac{2}{k}\right)^n \frac{1}{r^n} \gamma\left(n, \frac{r^2}{w_0^2 + 2iz/k}\right). \tag{11}$$

It is a straightforward task to verify that  $\Phi$  in this form satisfies the paraxial equation (4).

An independent and very simple way of deriving formula (11) is based on the method proposed in our earlier work [34], exploiting the Hankel transform [37,38], especially adapted to problems manifesting cylindrical symmetry. It was demonstrated there that a number of various beams of that kind can be derived from the single formula

$$\Phi(r, z) = \int_0^\infty ds s J_n(rs) \beta_n(s) e^{-\alpha(z)s^2/4}, \tag{12}$$

where  $\alpha(z) = w_0^2 + 2iz/k$ , by a proper choice of the function  $\beta(s)$ . Then it was observed that by picking this function in the form

$$\beta_n(s) = s^{n-2}, \quad \text{where } n = 2, 3, \dots, \tag{13}$$

one obtains the desired expression. After completing the integral with respect to  $s$ , this choice yields the result

$$\Phi(r, z) = 2^{n-1} \frac{1}{r^n} \gamma\left(n, \frac{r^2}{\alpha(z)}\right), \tag{14}$$

which is identical to (11) apart from the overall normalization constant. These results might naturally be obtained directly using, for example, the computational program MATHEMATICA [39]. In order to fix the constant, we require that

$$\begin{aligned} \int d^2r |\psi(r, z)|^2 &= \int_0^\infty dr r \int_0^{2\pi} d\varphi |\psi(r, \varphi, z)|^2 \\ &= 2\pi \int_0^\infty dr r |\Phi(r, z)|^2 = 1. \end{aligned} \tag{15}$$

In fact the calculation can be made easier by setting  $z = 0$ . The conservation of the value of this integral along the beam axis is guaranteed by the form of the paraxial equation (2) which is identical to the Schrödinger equation for a free particle in two spatial dimensions, with  $z$  playing the role of time. Moving along the  $z$  axis corresponds then to the temporal evolution in quantum mechanics and independence of (15) of  $z$  represents in fact the probability conservation condition. If so, the radial integral (without the inessential constants) can be boiled down to

$$\begin{aligned} \int_0^\infty dr r^{1-2n} \gamma\left(n, \frac{r^2}{w_0^2}\right) &= \frac{w_0^{2-2n}}{2} \int_0^\infty d\xi \xi^{-n} \gamma^2(n, \xi) \\ &= 2^{n-2} w_0^{2-2n} \Gamma(n-1), \end{aligned} \tag{16}$$

where the integration variable has been changed to  $\xi = r^2/w_0^2$ . Finally the normalized envelope of the  $\gamma$  beam can be written as

$$\begin{aligned} \Psi(r, \varphi, z, t) &= \frac{(\sqrt{2}w_0)^{n-1}}{\sqrt{\pi(n-2)!}} e^{ik(ct-z)} e^{in\varphi} \\ &\times \frac{1}{r^n} \gamma\left(n, \frac{r^2}{w_0^2(1 + iz/z_R)}\right), \end{aligned} \tag{17}$$

where the quantity  $z_R$  acts as the so-called Rayleigh length for a certain hypothetical Gaussian beam of the waist  $w_0$ , i.e.,

$$z_R = \frac{1}{2} k w_0^2. \tag{18}$$

These expressions will provide the starting point for further analysis in the following sections.

Some insight into the behavior of the beam can be gained by using the explicit form of the function  $\gamma(n, w)$  which applies for natural  $n$  [36]:

$$\gamma(n, w) = \Gamma[n] \left(1 - e^{-w} \sum_{j=0}^{n-1} \frac{w^j}{j!}\right). \tag{19}$$

It entails that the function  $\Psi(r, \varphi, z, t)$  is a sum of several Gaussian-like terms and of a power expression of  $r^{-n}$ . Nonetheless, none of these Gaussian-looking expressions individually is a solution to the paraxial equation nor represents

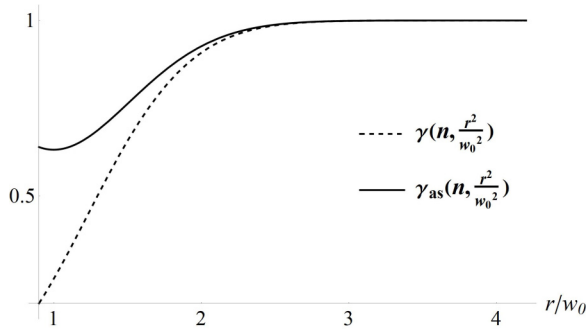


FIG. 1. The comparison of the approximate expression  $\gamma_{\text{as}}(n, \frac{r^2}{w_0^2})$  (solid line) with the exact one, i.e.,  $\gamma(n, \frac{r^2}{w_0^2})$  (dashed line), as functions of the radial distance from the beam's core for  $n = 2$ .

any Gaussian mode, which implies that (17) actually represents a different type of a beam.

It may be readily checked that for small arguments (i.e.,  $|w|$ ) the  $\gamma$  function can be approximated with

$$\gamma(n, w) \sim \frac{w^n}{n}, \quad (20)$$

which implies that close to the propagation axis the beam exhibits behavior typical for a vortex core of order  $n$ , i.e.,

$$\psi(r, \varphi, z) \sim \frac{r^n}{\alpha(z)^n} e^{in\varphi}. \quad (21)$$

On the other hand for large arguments it is obvious from (19) that

$$\gamma(n, w) \sim \gamma_{\text{as}}(n, w) := \Gamma(n) - w^{n-1} e^{-w}, \quad (22)$$

where “as” stands for “asymptotic.”

To ascertain at what distance from the axis the  $\gamma$  beam may be described with the use of (22), in Fig. 1 the quantities  $\gamma_{\text{as}}(n, \frac{r^2}{w_0^2})$  and  $\gamma(n, \frac{r^2}{w_0^2})$  are simultaneously plotted as functions of the radial variable  $r$  for the exemplary value of  $n = 2$ . It can be concluded that already for  $r > 2w_0$  the asymptotic expression can be used with good accuracy. In parallel, one can see that the first term in (22), i.e.,  $\Gamma(n)$ , is dominant, as the solid line gets almost flat (actually the second term contributes less than 7% at  $r = 2w_0$  and is very quickly decreasing with  $r$ ), leading to power-law decay of the function  $\Psi$  with growing  $r$ . For larger values of  $n$ , e.g., for  $n = 10$ , the distance at which  $\gamma_{\text{as}}$  fits for use increases slightly but does not exceed  $4w_0$ .

In [34] it was demonstrated that various choices of the function  $\beta_n(s)$  under the integral (12) lead to different paraxial beams possessing cylindrical symmetry. The particular choice in the form of (13) results, as we know, in the  $\gamma$  beam. As is obvious from this approach, it constitutes something like a “primitive” beam, or a “parent” beam, for a Gaussian and so-called elegant Laguerre-Gauss (eLG) beams. Accordingly, these three types of beams can be treated as belonging to a single family. As we know from [34], the functions  $\beta_n(s)$  generating these two latter beams assume the following forms:

$$\beta_n(s) = s^n, \quad \text{G beams}, \quad (23a)$$

$$\beta_n(s) = s^{n+2p}, \quad \text{eLG beams}, \quad (23b)$$

where  $n, p \in \mathbb{N}$ .

A close inspection of Eq. (12) suggests that these expressions can be generated if this inverse Hankel integral representing the  $\gamma$  beam gets differentiated an adequate number of times with respect to  $\alpha$ , or better yet, over  $z$ . One has then the following scheme (all beams here are of the same vorticity  $n$ ):

$$\gamma \text{ beam} \xrightarrow{\frac{\partial}{\partial z}} \text{G beam} \xrightarrow{\left(\frac{\partial}{\partial z}\right)^p} \text{eLG beam}. \quad (24)$$

This is confirmed by direct computation with the use of the formula

$$\frac{d}{dw} \gamma(n, w) = w^{n-1} e^{-w}, \quad (25)$$

which, after elementary transformations, yields

$$\frac{\partial}{\partial z} \psi_\gamma^{(n)}(r, \varphi, z) = C_0^{(n)} \psi_G^{(n)}(r, \varphi, z). \quad (26)$$

One could then say that the  $\gamma$  beam is more “fundamental” than the “fundamental Gaussian beam.”

A similar formula for eLG beams reads

$$\frac{\partial^{p+1}}{\partial z^{p+1}} \psi_\gamma^{(n)}(r, \varphi, z) = C_p^{(n)} \psi_{\text{eLG}(p)}^{(n)}(r, \varphi, z), \quad (27)$$

with  $C_0^{(n)}$  and  $C_p^{(n)}$  standing for some normalization constants since the normalization in the transverse plane is not preserved in the course of differentiation.

The results expressed in (26) and (27) constitute a pleasant property, but as a matter of fact it is not surprising that by computing derivatives with respect to  $z$  different solutions of Eq. (2) are produced. This is due to the fact that the paraxial operator has a vanishing commutator with  $\partial_z$  [40]:

$$\left[ \partial_r^2 + \frac{1}{r} \partial_r - \frac{n^2}{r^2} + 2ik\partial_z, \partial_z \right] = 0. \quad (28)$$

Naturally exact expressions for G and eLG beams with  $n < 2$  cannot be generated that way, as the corresponding  $\gamma$  beam does not exist. It should be mentioned that certain differential relations between the fundamental Gaussian mode and the Hermite-Gauss or Laguerre-Gauss modes have already been exploited (see, e.g., [41,42]). However, formula (12), if applicable, makes this kind of relationship trivially simple.

The above property implies a useful result based on the usual Taylor expansion:

$$\begin{aligned} e^{ik\Delta z} \Psi_\gamma^{(n)}(r, \varphi, z + \Delta z, t) - \Psi_\gamma^{(n)}(r, \varphi, z, t) \\ = C_0^{(n)} \Delta z \Psi_G^{(n)}(r, \varphi, z, t) \\ + \sum_{p=1}^{\infty} \frac{C_p^{(n)}}{(p+1)!} \Delta z^{p+1} \Psi_{\text{eLG}(p)}^{(n)}(r, \varphi, z, t), \end{aligned} \quad (29)$$

which implies that the propagation of the  $\gamma$  beam along the  $z$  axis is determined by the values assumed by the corresponding G and eLG beams at a given arbitrarily chosen point (for instance at the beam's waist). Taking the derivative of both sides of (29) with respect to  $\Delta z$  a similar expansion for the Gaussian mode in terms of eLG modes can be easily derived.

Formula (29) states in fact that a wave resulting from the superposition of two arbitrarily shifted  $\gamma$  beams with appropriately chosen relative phases regains the Gaussian form in

the transverse plane due to the destructive interference. This in turn reflects the fact, referred to earlier, that the asymptotic “tails” are  $z$  independent.

### III. PARAMETERS OF $\gamma$ BEAMS

#### A. Beams with $n \geq 3$

From (22) it is obvious that unlike typical beams the intensity profile does not display the Gaussian character. Already at the distance of few  $w_0$  from the propagation axis the dominating term exhibits the power-law falloff. This means that the parameters that are commonly used to characterize a beam (its waist, radius, Rayleigh length, etc.) cannot be read off directly from the exponential factor and need to be redefined.

In order to obtain the expression for the analog of the beam radius, commonly denoted with  $w(z)$ , it is convenient to calculate

$$\langle r^2 \rangle_z = \int d^2r |r|^2 \cdot |\Psi(\mathbf{r}, z, t)|^2. \quad (30)$$

This two-dimensional integration is performed only in the transverse plane, and the normalized wave function in cylindrical coordinates is taken from (17). The convergence at the origin is assured by the mentioned behavior of the  $\gamma$  function for small arguments [see Eq. (20)], and at infinity (for  $n > 2$ ) by the denominator  $1/r^n$ . The subscript  $z$  indicates that this quantity is  $z$  dependent, as we are dealing with a diffracting beam. Obviously, the time dependence disappears in (30).

Then the  $\gamma$ -beam radius is defined in a natural way as

$$w_\gamma(z) = [\langle r^2 \rangle_z]^{1/2}. \quad (31)$$

This seems a reasonable generalization, since for a pure Gaussian of the type  $\exp(-r^2/r_0^2)$  one would obtain that way  $[\langle r^2 \rangle]^{1/2} = r_0$ .

In order to calculate this value we first consider the auxiliary integral:

$$I(\zeta) = \int_0^\infty dx x^{1-n} \gamma\left(n, \frac{x}{1+i\zeta}\right) \gamma\left(n, \frac{x}{1-i\zeta}\right), \quad (32)$$

where  $\zeta$  stands for a certain real parameter. Now  $I(\zeta)$  can be found by differentiating both sides with respect to  $\zeta$ ,

$$\begin{aligned} \frac{dI}{d\zeta} = -i \left[ \frac{1}{(1+i\zeta)^{n+1}} \int_0^\infty dx x e^{-x/(1+i\zeta)} \gamma\left(n, \frac{x}{1-i\zeta}\right) \right. \\ \left. - (\zeta \mapsto -\zeta) \right], \end{aligned} \quad (33)$$

where the explicit formula for  $\gamma'(n, w)$  has been used:

$$\gamma'(n, w) = w^{n-1} e^{-w}. \quad (34)$$

Now, integrating by parts, one can “kill” the  $\gamma$  function, obtaining an elementary integral:

$$\begin{aligned} \frac{dI}{d\zeta} = -\frac{i}{2^n} (1+i\zeta) \left[ \int_0^\infty dx \left( \frac{1}{2} (1-i\zeta)x^n + x^{n-1} \right) e^{-x} \right. \\ \left. - (\zeta \mapsto -\zeta) \right], \end{aligned} \quad (35)$$

where some obvious and straightforward transformations have been omitted. Finally one comes to the needed formula:

$$I'(\zeta) = \frac{(n-1)!}{2^{n-1}} \zeta \implies I(\zeta) = \frac{(n-1)!}{2^n} \zeta^2 + I(0), \quad (36)$$

with  $I(0)$  easily fixed to

$$I(0) = \int_0^\infty dx x^{1-n} \gamma^2(n, x) = \frac{(n-1)!(n+2)}{2^n(n-2)}. \quad (37)$$

Now returning to the formula (31) with  $\Psi$  given by (17), one can readily observe that the simple substitution  $r^2 = x w_0^2$  leads to the following result:

$$\begin{aligned} w_\gamma(z) &= w_0 \left[ \frac{2^{n-1}}{(n-2)!} I\left(\frac{z}{z_R}\right) \right]^{1/2} \\ &= w_0 \left[ \frac{n-1}{2} \left( \frac{n+2}{n-2} + \frac{z^2}{z_R^2} \right) \right]^{1/2}. \end{aligned} \quad (38)$$

This reveals the hyperbolic law of variation with  $z$  typical of solutions of the paraxial equations [43,44].

For the beam dealt with in the present paper, the defined parameters such as  $w_\gamma(z)$  and others given below will bear the additional subscript  $\gamma$  unlike those describing a Gaussian beam. First, it is obvious from (38) that the waist is now given as

$$w_{0\gamma} := w_\gamma(0) = w_0 \sqrt{\frac{(n-1)(n+2)}{2(n-2)}}, \quad (39)$$

and increases with  $n$ , but the smallest value is assumed for  $n = 4$  ( $w_{0\gamma} \approx 2.12 w_0$ ). Second, the new Rayleigh length  $z_{R\gamma}$  can be found from the condition

$$\frac{w_\gamma(z_{R\gamma})}{w_{0\gamma}} = \sqrt{2}, \quad (40)$$

leading to

$$z_{R\gamma} = z_R \sqrt{\frac{n+2}{n-2}}. \quad (41)$$

As  $n$  increases starting from  $n = 3$ ,  $z_{R\gamma}$  declines from its initial value of  $\sqrt{5} z_R$  to  $z_R$ , which reflects the growing diffraction effects. The relatively long distance  $\sqrt{5} z_R$  is related to the larger spot size. What is interesting is that the smallest value of  $w_{0\gamma}$  (for  $n = 4$ ) does not necessarily correspond to the shortest length  $z_{R\gamma}$ .

Using the above expressions the formula for the beam's radius may now be given the familiar form

$$w_\gamma(z) = w_{0\gamma} \sqrt{1 + \frac{z^2}{z_{R\gamma}^2}}, \quad (42)$$

but one has to remember that both  $w_{0\gamma}$  and  $z_{R\gamma}$  are here  $n$  dependent.

The divergence half angle of the beam is defined as

$$\begin{aligned} \tan \theta_{0\gamma} \approx \theta_{0\gamma} &= \lim_{z \rightarrow \infty} \frac{w_\gamma(z)}{z} = \frac{w_{0\gamma}}{z_{R\gamma}} \\ &= \sqrt{\frac{n-1}{2}} \frac{w_0}{z_R} = \sqrt{\frac{n-1}{2}} \theta_0, \end{aligned} \quad (43)$$

where  $2\theta_0$  represents the divergence angle of the Gaussian beam. It should be noted that in the case of the least diverging beam (i.e., for  $n = 3$ )  $\theta_{0\gamma} = \theta_0$ .

Finally one can define a number quantifying the beam quality [45,46], namely,

$$\mathbb{M}_\gamma^2 = \frac{\pi w_{0\gamma} \theta_{0\gamma}}{\lambda} = \frac{n-1}{2} \sqrt{\frac{n+2}{n-2}} \mathbb{M}^2 = \frac{n-1}{2} \sqrt{\frac{n+2}{n-2}}, \quad (44)$$

since for the Gaussian beam  $\mathbb{M} = 1$ . The “best” situation occurs again for  $n = 3$  for which  $\mathbb{M}_\gamma = 5^{1/4} \approx 1.5$ .

### B. The special case of $n = 2$

A nontruncated  $\gamma$  beam with the vorticity  $n = 1$  does not exist as it would transport an infinite amount of energy. Beams with  $n \geq 3$  have been characterized in the previous subsection. One is then left with the case of  $n = 2$ , for which the integral (30) would diverge, and thus the necessary parameters need to be defined in a different way. In this case it seems natural to calculate

$$\langle r \rangle_z = \int d^2r |r| \cdot |\Psi(\mathbf{r}, z, t)|^2. \quad (45)$$

This integral is more challenging to calculate in view of the “inconvenient” power of  $r$ , but it does converge, since at infinity the integrand function depends on the radial variable as  $r^{-3}$ . In order not to bore the reader with the details of calculating this integral, only the final result will be provided:

$$w_\gamma(z) := \langle r \rangle_z = \sqrt{8\pi} w(z) \left[ \frac{1}{8} + \frac{w_0}{w(z)} \sqrt{1 + \frac{w_0}{w(z)}} - \frac{w_0^2}{w(z)^2} \right], \quad (46)$$

where  $w_0$ ,  $w(z) = w_0 \sqrt{1 + z^2/z_R^2}$ , and  $z_R$  given by (18), are again quantities related to a Gaussian beam. It should be pointed out that the quantities redefined in the present subsection, bearing an additional index  $\gamma$  [as for example  $w_\gamma(z)$ ], and referring solely to the case of  $n = 2$ , are only applicable here, and in later sections of this paper, unless explicitly stated, the general formulas previously defined for  $n \geq 3$  apply.

Expression (46) cannot be given a concise form similar to (42). However, the minimal value of  $w_\gamma(z)$  is still obtained at  $z = 0$ , since the derivative of  $w_\gamma(z)$  has there the only root, which corresponds to a minimum. In order to define  $w_{0\gamma}$  we calculate then

$$w_{0\gamma} := w_\gamma(0) = \sqrt{\pi} \left( 4 - \frac{7\sqrt{2}}{4} \right) w_0 \approx 2.7w_0. \quad (47)$$

This result is by no means surprising as  $\Psi$  decays very weakly in the radial direction (merely as  $r^{-2}$ ) so the beam’s intensity is distributed in a broader region.

For large  $z$ , the beam’s width exhibits typical linear behavior:

$$w_\gamma(z) \approx \sqrt{\frac{\pi}{8}} \frac{w_0}{z_R} z, \quad (48)$$

which shows that the slope is about 0.63 of that which appears for the Gaussian beam (i.e.,  $w_0/z_R$ ). The new Rayleigh length

is derived from the condition (40), which now reads

$$\sqrt{1 + \zeta^2} + 8 \sqrt{1 + \frac{1}{\sqrt{1 + \zeta^2}}} - \frac{8}{1 + \zeta^2} = 16 - 7\sqrt{2}, \quad (49)$$

where, in order to make the expression more condensed, the symbol  $\zeta = z_{R\gamma}/z_R$  has been introduced. Only numerical solution of (49) is possible, and one gets

$$z_{R\gamma} \approx 0.58 z_R. \quad (50)$$

These results allow us to estimate the beam’s divergence and quality:

$$\tan \theta_{0\gamma} \approx \theta_{0\gamma} = \sqrt{\frac{\pi}{8}} \frac{w_0}{z_R} = \sqrt{\frac{\pi}{8}} \theta_0 \approx 0.63 \theta_0, \quad (51a)$$

$$\mathbb{M}_\gamma^2 = \pi \left( \sqrt{2} - \frac{7}{8} \right) \mathbb{M}^2 \approx 1.67 \implies \mathbb{M} \approx 1.29. \quad (51b)$$

From that point of view, the beam for  $n = 2$  turns out to be “better” (but simultaneously broader) than that found in the previous subsection.

## IV. INTENSITY AND PHASE

The local beam’s intensity may be characterized by the function

$$|\Psi(r, \varphi, z, t)|^2 = \frac{(2w_0^2)^{n-1}}{\pi(n-2)! r^{2n}} \left| \gamma \left( n, \frac{r^2}{w_0^2(1 + iz/z_R)} \right) \right|^2, \quad (52)$$

which vanishes both for  $r \rightarrow 0$  and  $\infty$ . Owing to (20) close to the propagation axis the following approximation holds:

$$|\Psi(r, \varphi, z, t)|^2 \approx \frac{2^{n-1}}{\pi n^2 (n-2)! w_0^2} \left( \frac{r^2}{w_0^2(1 + z^2/z_R^2)} \right)^n. \quad (53)$$

A similar formula for a Gaussian beam would have the additional power of  $(1 + z^2/z_R^2)$  in the denominator. For large  $r$ , as stems from (22), the leading term is  $z$  independent, and reads

$$|\Psi(r, \varphi, z, t)|^2 \approx \frac{2^{n-1}(n-1)(n-1)!}{\pi w_0^2} \left( \frac{w_0^2}{r^2} \right)^n. \quad (54)$$

In Fig. 2 the contour plots of  $|\Psi(r, \varphi, z, t)|^2$  are depicted in the exemplary plane  $z = 0.1 z_R$  for  $n = 2$  [left plot (a)],  $n = 10$  [left plot (b)], and  $n = 30$  [left plot (c)]. The accompanying figures on the right illustrate the dependence of  $|\Psi|^2$  on the radial variable  $r$  along with the corresponding Gaussian beams. It should be recalled, however, that the expressions describing the  $\gamma$ -beam irradiance have yet slowly vanishing “tails,” hardly visible in the figures but contributing substantially to the integrals for the beam’s radius.

The convention adopted throughout the paper is that the scale on the axes is specified by the parameters  $w_0$ , or  $z_R$ , rather than  $w_{0\gamma}$  or  $z_{R\gamma}$ . As we recall, the latter are functions of  $n$ , so one would have different scales in each of the figures, making their easy comparison impossible.

The left column of Fig. 3, in turn, displays the same quantity in the plane comprising the propagation axis for increasing values of the parameter  $n$  (2, 3, 5, 10, and 20). The right column provides the same diagrams with the additional lines

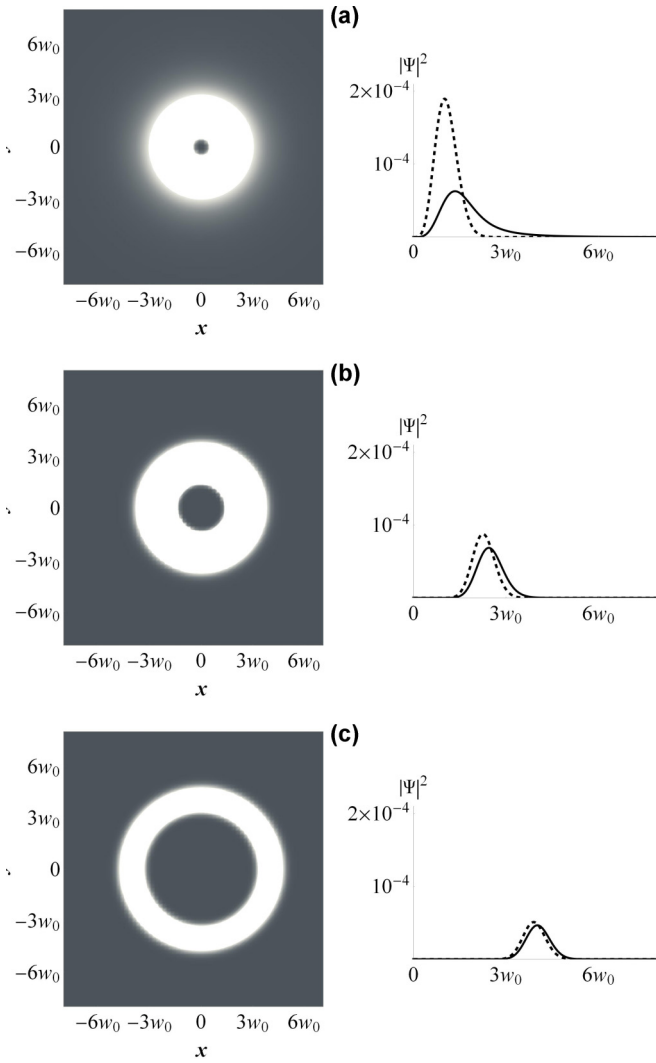


FIG. 2. The intensity distribution of the  $\gamma$  beam in the plane  $z = 0.1z_R$  for (a)  $n = 2$ , (b)  $n = 10$ , and (c)  $n = 30$ . The left column plots represent the wave intensities in grayscale starting from low intensity (dark) to high intensity (bright). In the right column the corresponding normalized value of  $|\Psi|^2$  [in units  $(2\pi/\lambda)^2$ ] is plotted as a function of the radial distance  $r$  (solid lines). For comparison the same quantity is plotted for the appropriate Gaussian beam (dashed lines).

representing the values of  $w(z)$  and  $w_\gamma(z)$  imprinted on them. For the latter, either formula (38) or (46) was used depending on the value of  $n$ . Dark colors have been lightened slightly relative to the previous figure in order to make the additional lines and captions on the axes better visible.

A couple of observations can be made. First, contrary to  $w(z)$ , the calculated quantity  $w_\gamma(z)$  well corresponds to the surface of the high-energy concentration, represented by light regions: the larger  $n$  is dealt with, the better is the agreement. The reason for it can already be seen in Fig. 2: for high  $n$  the beam is more focused around areas of high irradiance, for smaller  $n$  more dilution occurs. Secondly, a bigger  $n$  correlates to a larger waist and to a wider beam, which might also be inferred from the formulas for  $w_\gamma(z)$ . Finally, at a distance of one to two  $z_R$  (i.e., about  $z_{R\gamma}$ ) there occurs a visible dilution

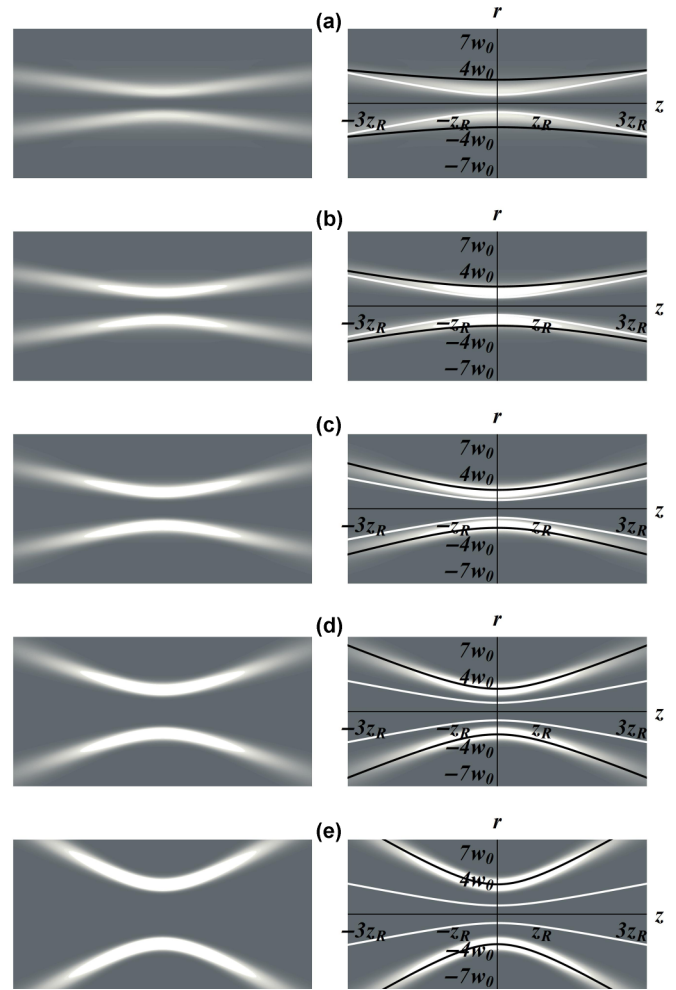


FIG. 3. The intensity distribution of the  $\gamma$  beam in the plane containing the wave propagation axis for (a)  $n = 2$ , (b)  $n = 3$ , (c)  $n = 5$ , (d)  $n = 10$ , and (e)  $n = 20$ . The left column and the right one show the same distribution, but the diagrams on the right include in addition the axial intersections of the surfaces  $w(z)$  (white lines) and  $w_\gamma(z)$  (black lines). For better visibility the grayscale is slightly brightened up relative to Fig. 2.

of the irradiance, i.e., not a transverse expansion of the beam, which at a distance of  $z_{R\gamma}$  takes place by the factor of  $\sqrt{2}$  by definition, but a clear weakening of the energy concentration areas. This is shown in Fig. 4 for  $z = 0$ ,  $z_R$ , and  $2z_R$ .

Moving on to the beam's phase, it should be noted that due to the asymptotic behavior of the  $\gamma$  function the phase at large radial distances is determined solely by the factor  $e^{i(kz+n\varphi)}$  (omitting the factor  $e^{-ikt}$  which merely leads to a global rotation of the whole structure). Therefore, in each plane  $z = \text{const}$ , the lines of constant phase are (asymptotically) radially oriented unlike, for instance, the Gaussian beam, for which they assume a spiral character. This pattern with growing  $r$  was due to the presence of the  $r$ -dependent factor  $e^{ikr^2/R(z)}$  (see for instance [22]) which does not emerge in the case of  $\gamma$  beams. The additional helical twist produced by the interplay of  $z$  and  $\varphi$ , typical for any vortexlike beam, appears when moving along the propagation axis and does not manifest itself in any individual plane.

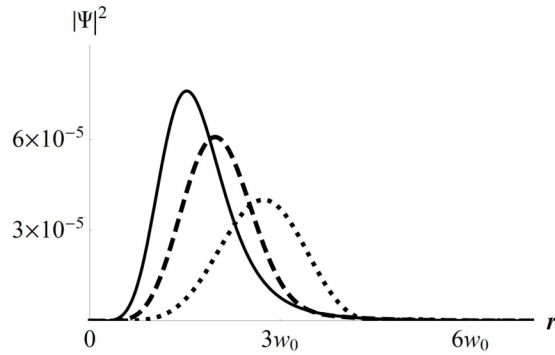


FIG. 4. The normalized value of  $|\Psi|^2$  [in units  $(2\pi/\lambda)^2$ ] for  $n = 3$  plotted as a function of the radial distance  $r$  at  $z = 0$  (solid line),  $z = z_R$  (dashed line), and  $z = 2z_R$  (dotted line).

In Fig. 5, the phases of the Gaussian beam (upper plots) and of the  $\gamma$  beam (lower plots) are compared in two planes:  $z = 0$  and  $2.24 z_R$ . This latter value is chosen, since it corresponds to  $z_{R\gamma}$  for  $n = 3$ .

In the lower, right diagram, the mentioned effects can be observed. Asymptotically, the curve of constant phase tends really to a straight line (white dashed line), directed radially. One can estimate its rotation angle relative to the direction of the tangent line close to the origin (black dashed line). From the asymptotic behavior discussed earlier, it is evident that the

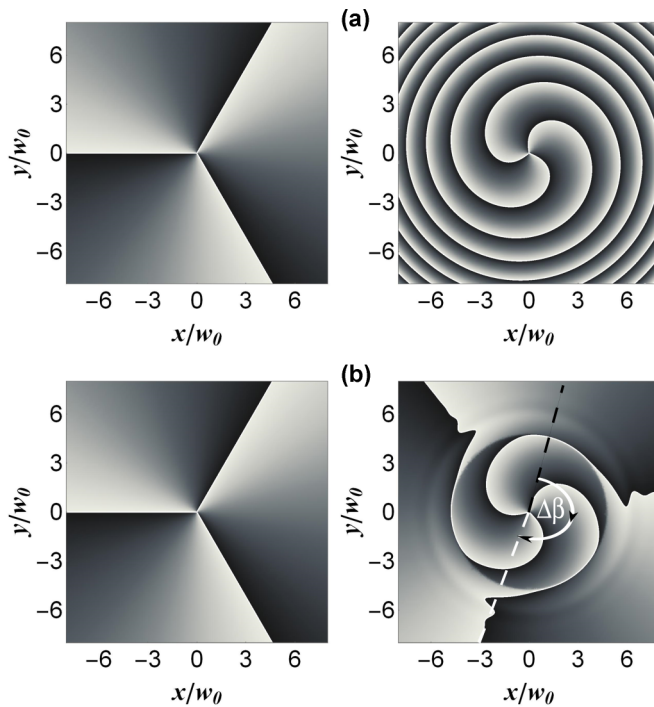


FIG. 5. The phases of (a) the Gaussian beam and (b) the  $\gamma$  beam, for  $n = 3$ , depicted in two planes:  $z = 0$  and  $2.24 z_R$ . The value of the phase, modulo  $2\pi$ , is represented continuously by means of the grayscale from  $-\pi$  (black color) to  $\pi$  (white color). The dashed semilines show the directions of the tangent line at the origin (black line) and that at infinity (white line). It is seen that  $\Delta\beta \gtrsim \pi$ .

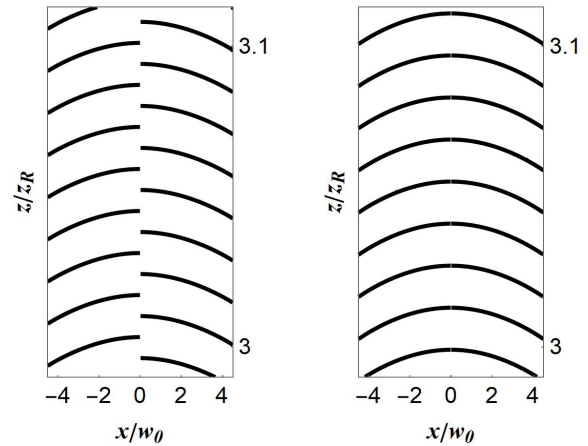


FIG. 6. The intersection of wavefronts of two  $\gamma$  beams with the axial plane  $xz$  for  $n = 3$  (left plot) and  $n = 4$  (right plot). The wavefront surfaces are drawn for integer values of  $\pi$ .

additional phase factor reads

$$e^{-i\Delta\beta} := e^{-in \arctan \frac{z}{z_R}} = e^{-in\psi_G(z)}, \quad (55)$$

where  $\psi_G(z)$  stands for the so-called Gouy phase of a Gaussian beam with Rayleigh distance  $z_R$  [22]. By substituting  $z/z_R = 2.24$  and  $n = 3$ , this angle becomes  $-3.45$  rad. This value is close to  $\pi$ , so the semilines in the figure point in almost opposite directions.

In Fig. 6 the intersection of the surfaces “phase = 0” and “phase =  $\pi$ ” with the axial plane  $y = 0$  is presented for  $n = 3$  and 4. The typical situation for odd values of  $n$  is shown in the left diagram. The rotation around the  $z$  axis generates the phase factor which is a multiplicity of  $2\pi$  plus additional  $\pi$ . Consequently the contours are discontinuous (the true three-dimensional surfaces of constant phase are of course continuous). In contrast, the second plot (for even  $n$ ) does not show any discontinuities since the rotation about the  $z$  axis generates the additional phase factor of  $e^{in\pi}$  which equals 1 for even  $n$ .

## V. SUMMARY

A family of cylindrical paraxial beams, called in this paper “ $\gamma$  beams,” has been constructed in an analytical way, by a direct solution of the scalar paraxial equation. An independent method of obtaining the analytical expression, developed in [34], is based on the Hankel transform. These modes are endowed with vorticity  $n$ , with  $n \geq 2$ . For  $n = 0$  or 1 such beams cannot be constructed, because they would carry an infinite amount of energy. The spatial profile is described by an incomplete gamma function, hence the name “ $\gamma$  beam.” From the asymptotic properties of this function, it follows that at distances of the order of few  $w_0$  such a beam is not Gaussian in nature, but falls off in a power-law fashion as  $1/r^n$ . From the derivation it follows that the  $\gamma$  beams constitute a sort of parent beam for Gaussian and elegant Laguerre-Gauss beams, which may, thereby, be referred to as “daughter” beams. The formulas for the parameters describing this kind of a beam cannot be read off from the Gaussian

factor, which is not present. Therefore, they have been defined and obtained independently. The intensity distribution of the wave and its phase in the transverse plane have been analyzed and illustrated in the figures. The intensity profile shows a single annular maximum with a  $z$ -dependent radius corresponding to the theoretically derived beam's size  $w_\gamma(z)$ . The wave phase exhibits a different spatial character than that of

generic Gaussian beams, for which the lines of constant phase in a plane perpendicular to the propagation direction have a spiral pattern. In contrast, in a  $\gamma$  beam these lines tend to radial asymptotes. As to the practical realization, it seems that the most direct method of generating  $\gamma$  beams might be the use of a computer-generated hologram or computer-controlled spatial light modulator.

- 
- [1] D. J. Stevenson, F. J. Gunn-Moore, and K. Dholakia, *J. Biomed. Opt.* **15**, 041503 (2010).
- [2] F. M. Fazal and S. M. Block, *Nat. Photon.* **5**, 318 (2011).
- [3] *Optical Tweezers: Methods and Applications*, edited by M. Padgett, J. Molloy, and D. McGloin, Series in Optics and Optoelectronics (CRC, Boca Raton, FL, 2010).
- [4] M. Woerdemann, *Structured Light Fields: Applications in Optical Trapping, Manipulation, and Organisation* (Springer-Verlag, Berlin, 2012).
- [5] R. W. Bowman and M. J. Padgett, *Rep. Prog. Phys.* **76**, 026401 (2013).
- [6] D. G. Grier, *Nature (London)* **424**, 810 (2003).
- [7] V. Kollárová, T. Medřík, R. Čelechovský, Z. Bouchala O. Wilfert, and Z. Kolka D.D.S., *Proc. SPIE* **6736**, 368 (2007).
- [8] C. Altucci, R. Bruzzese, D. D'Antuoni, C. de Lisio, and S. Solimeno, *J. Opt. Soc. Am. B* **17**, 34 (2000).
- [9] M. Nisoli, E. Priori, G. Sansone, S. Stagira, G. Cerullo, S. De Silvestri, C. Altucci, R. Bruzzese, C. de Lisio, P. Villorosi, L. Poletto, M. Pascolini, and G. Tondello, *Phys. Rev. Lett.* **88**, 033902 (2002).
- [10] H. Sasada and M. Okamoto, *Phys. Rev. A* **68**, 012323 (2003).
- [11] L. C. Comandar, M. Lucamarini, B. Fröhlich, J. F. Dynes, A. W. Sharpe, S. W.-B. Tam, Z. L. Yuan, R. V. Pentyl, and A. J. Shields, *Nat. Photon.* **10**, 312 (2016).
- [12] T. Radożycki, *Phys. Rev. A* **102**, 063101 (2020).
- [13] L. W. Davis and G. Patsakos, *Opt. Lett.* **6**, 22 (1981).
- [14] A. E. Siegman, *Lasers* (University Science, Mill Valley, 1986).
- [15] S. Nemoto, *Appl. Opt.* **29**, 1940 (1990).
- [16] L. Mandel and E. Wolf, *Optical Coherence and Quantum Optics* (Cambridge University, New York, 1995).
- [17] I. Białynicki Birula and Z. Białynicka Birula, *J. Phys. A* **46**, 053001 (2013).
- [18] S. R. Seshadri, *J. Opt. Soc. Am. A* **15**, 2712 (1998).
- [19] G. Rodríguez-Morales and S. Chávez-Cerda, *Opt. Lett.* **29**, 430 (2004).
- [20] S. V. Ershkov, *J. King Saud Univ. Sci.* **27**, 198 (2015).
- [21] M. V. Selina, *J. Opt.* **49**, 338 (2020).
- [22] B. E. A. Saleh and M. C. Teich, *Fundamentals of Photonics* (Wiley, New York, 2007).
- [23] F. Gori, G. Guattari, and C. Padovani, *Opt. Commun.* **64**, 491 (1987).
- [24] A. April, *J. Opt. Soc. Am. A* **28**, 2100 (2011).
- [25] J. Mendoza-Hernández, M. L. Arroyo-Carrasco, M. D. Iturbe-Castillo, and S. Chávez-Cerda, *Opt. Lett.* **40**, 3739 (2015).
- [26] V. Bagini, F. Frezza, M. Santarsiero, G. Schettini, and G. Schirripa Spagnolo, *J. Mod. Opt.* **43**, 1155 (1996).
- [27] Ch.-F. Li, *Opt. Lett.* **32**, 3543 (2007).
- [28] T. Radożycki, *Phys. Rev. A* **104**, 023520 (2021).
- [29] L. Allen, M. W. Beijersbergen, R. J. C. Spreeuw, and J. P. Woerdman, *Phys. Rev. A* **45**, 8185 (1992).
- [30] M. Padgett, J. Arlt, N. Simpson, and L. Allen, *Am. J. Phys.* **64**, 77 (1996).
- [31] A. April, *Opt. Lett.* **33**, 1392 (2008).
- [32] A. April, *Opt. Lett.* **33**, 1563 (2008).
- [33] W. Nasalski, *J. Opt.* **20**, 105601 (2018).
- [34] T. Radożycki, *Opt. Laser Technol.* **147**, 107670 (2022).
- [35] M. Lax, W. H. Louisell, and W. B. McKnight, *Phys. Rev. A* **11**, 1365 (1975).
- [36] J. Spanier and K. B. Oldham, *An Atlas of Functions* (Springer-Verlag, Berlin, 1987).
- [37] B. Patra, *An Introduction to Integral Transforms* (CRC, Boca Raton, FL, 2018).
- [38] A. Erdelyi, *Tables of Integral Transforms* (McGraw-Hill, New York, 1954), Vol. 2.
- [39] Wolfram Research, Inc., *Mathematica*, Champaign, IL, 2021.
- [40] A. Wünsche, *J. Opt. Soc. Am. A* **6**, 465 (1989).
- [41] E. Zauderer, *J. Opt. Soc. Am. A* **3**, 465 (1986).
- [42] J. Enderlein and F. Pampaloni, *J. Opt. Soc. Am. A* **21**, 1553 (2004).
- [43] F. Gori, M. Santarsiero, and A. Sona, *Opt. Commun.* **82**, 197 (1991).
- [44] M. A. Porrás, J. Alda, and E. Bernabeu, *Appl. Opt.* **31**, 6389 (1992).
- [45] A. E. Siegman, *Proc. SPIE* **1224**, 2 (1990).
- [46] A. E. Siegman, *Proc. SPIE* **1868**, 2 (1993).